

An Embedded Approach to the Implementation of a Multi-Agent Energy Management System for Unmanned Systems

Vadym Slyusar^{*†}, Serhii Pochernin^{*†}.

[†] Central Scientific Research Institute of Armaments and Military Equipment of the Armed Forces of Ukraine, Avenue of the Air Forces, 28, Kyiv, Ukraine, 03049

Abstract

The paper proposes a multi-agent energy management system for autonomous unmanned platforms, specifically unmanned aerial vehicles (UAVs) and unmanned ground robotic complexes (UGRCs). For the first time, an embedding-based approach is employed to represent the technical state of the battery pack: a multidimensional feature vector is mapped into an embedding space for subsequent analysis, classification, and prediction. The effectiveness of clustering and short-term degradation forecasting of battery cells-implemented via the embedding method using MLP models-is demonstrated. Simulation results confirm the feasibility of early detection of critical battery operating modes and adaptive energy management. The integration of the embedding approach within a multi-agent architecture is examined, assigning distinct roles to monitoring, classification, prediction, and decision-making agents. Attention is also given to the potential integration with digital twin models of batteries. The proposed method is suitable for deployment on edge devices and is promising for application in high-reliability power systems operating under resource-constrained and highly dynamic conditions.

Keywords

Lithium-based battery, health index, SoC, SoH, RUL, embedding vector, LSTM, MLP – prediction, battery diagnostics, power supply, multi-agent system, unmanned systems

1. Introduction

The energy autonomy of unmanned aerial vehicles (UAVs) and unmanned ground robotic complexes (UGRCs) critically depends on the ability to rapidly and reliably assess the residual operational capacity of their battery packs. Traditional methods, which rely on individual metrics (State of Charge (SoC), cell internal resistance, temperature, etc.) [1], fail to capture the full scope of degradation processes. In this work, we propose an integral health vector that unifies discrete performance indicators - SoC, State of Health (SoH), Remaining Useful Life (RUL), and other diagnostic features-and projects them into a multidimensional embedding space, thereby laying the groundwork for a multi-agent system (MAS) capable of real-time classification, prediction, and energy-management decision-making. Addressing the challenge of estimating the remaining useful life of batteries requires a systematic approach that spans the evolution of methods - from the analysis of individual physical parameters to the development of integrated digital representations. Accordingly, it is appropriate to examine the historical stages of scientific approaches that have established the modern foundation for embedding integration within multi-agent energy-decision support systems.

In [2], a cloud-based digital twin for batteries with online SoC/SoH estimation is proposed, demonstrating the promise of remote monitoring. The NASA dataset [3] has become a benchmark

ICST-2025: Information Control Systems & Technologies, September 24-26, 2025, Odesa, Ukraine.

* Corresponding author.

† These authors contributed equally.

✉ swadim@ukr.net (V. Slyusar); sergiomrc28@gmail.com (S. Pochernin);

ORCID 0000-0002-2912-3149 (V. Slyusar); 0000-0002-4804-3259 (S. Pochernin)



© 2025 Copyright for this paper by its authors. Use permitted under Creative Commons License Attribution 4.0 International (CC BY 4.0).

for modeling lithium-ion cell degradation. Study [4] presents an interpretable neural network model for SoH forecasting, affirming the feasibility of feature vectorization. The review in [5] systematizes BMS functionalities and emphasizes the need for comprehensive indicators and predictive capabilities. Study [6] demonstrated that the application of neural networks enhances RUL forecasting, whereas work [7] focuses on energy-efficient cooperative mission planning for drones under battery constraints, emphasizing the necessity of accurate flight-time predictions. Finally, [8] introduces a UAV-aided digital twin framework for IoT networks, corroborating the growing role of digital twins in the management of UAV fleets.

Neural network-based approaches to SoC estimation have been demonstrated in [9], while the deployment of predictive models on edge devices using transfer learning is described in [10]. To capture long-term nonlinear patterns, it is common to employ the Long Short-Term Memory (LSTM) architecture. [11] and attention mechanisms [12] have been employed, and deep ResNet models [13] have been shown to stabilize the training of complex networks. The survey in [14] summarizes hybrid (physics-informed statistical) battery models that enhance estimation accuracy. Finally, a scalable multi-agent architecture based on a “mixture-of-experts” paradigm for 6G networks is proposed in [15], highlighting the potential of distributed decision-making. Thus, the evolution from measuring individual metrics to employing integral embedding vectors and multi-agent systems represents a contemporary trend in the energy management of unmanned systems.

Regarding the perspectives for practical implementation, multi-agent energy management system find direct application in complex UAV missions where sustained operational efficiency is critical. For example, in swarm-based UAV operations for radio-electronic reconnaissance and active electronic warfare, as described in [16], energy allocation decisions must be made dynamically to ensure continuous jamming of adversary systems while maintaining reconnaissance coverage over designated areas. Such scenarios demand precise coordination of SoC, SoH, and RUL data across the swarm to prevent premature mission aborts. Similarly, MAS architectures can be integrated into UAV mission control frameworks for meteorological data collection in IoT-based environments [17] or optimized routing over rough terrain using machine learning [18], where energy-aware path planning directly influences mission success. Beyond tactical missions, MAS-based energy management can be embedded into logistics systems such as LOGFAS or ARK AI, enabling synchronized planning of UAV fleet deployments, predictive battery replacement scheduling, and integration of energy constraints into broader operational planning cycles. These practical implementations underscore the dual role of the proposed architecture - as both a tactical decision-support tool and a component of higher-level logistics and command systems - thereby bridging the gap between battery diagnostics, operational planning, and autonomous mission execution.

The following exposition demonstrates how the constructed health-assessment vector is mapped into the embedding space, how the agent architecture leverages this representation for clustering, prediction, and decision-making, and how the novel metrics enable aggregated diagnostics of battery condition in complex tactical scenarios.

2. Formation of the Battery Health Vector

The operation of modern autonomous platforms - namely unmanned aerial vehicles (UAVs) and unmanned ground vehicles (UGVs) - requires a reliable assessment of the residual capacity of their power sources. This analysis centers on three key performance indicators: State of Charge (SoC), State of Health (SoH), and Remaining Useful Life (RUL). Individually, these parameters inform on the current energy reserve, the extent of degradation, and the projected future lifespan, respectively. However, only when considered collectively do they provide a comprehensive “portrait” of the battery’s condition at a given moment.

2.1. Interrelationship of the SoC, SoH, and RUL Performance Indicators

Presented below is a concise overview of the most widely adopted and complementary metrics enabling quantitative evaluation of lithium-based battery performance across its entire life cycle. The State of Charge (SoC) metric defines the percentage level of available capacity within the current cycle:

$$SoC(t) = \frac{Q(t)_{aval.}}{Q_{nom}}. \quad (1)$$

In practice, it is computed by coulomb counting - that is, integrating the current over time-and subsequently corrected using open-circuit voltage (OCV) calibration. This approach maintains an error below 1 % even under dynamic loading and temperature variations [19].

On the other hand, the State of Health (SoH) describes the long-term degradation of the battery and has several equivalent formulations:

$$SoH_c(t) = \frac{C_{max}(t)}{C_{init}}, \quad (2)$$

$$SoH_R(t) = \frac{R_{EOL} - R_0}{R_{EOL} - R(t)_{init}}. \quad (3)$$

The capacity-based indicator $SoH_c(t)$ (2) is defined as the ratio of the actual measured capacity to the initial capacity, reflecting the loss of active lithium mass. The impedance-based indicator $SoH_R(t)$ (3) reflects the progressive increase of internal resistance during battery aging and is commonly defined using the end-of-life resistance R_{EOL} , corresponding to the failure threshold, and the initial resistance $R(t)_{init}$ [20]. For the assessment of the remaining “lifetime” resource-typically expressed in cycles or operating hours until the failure threshold is reached-the Remaining Useful Life (RUL) metric is applied [20]:

$$RUL(t) = t_{EOL} - t_{init}, \quad (4)$$

where t_{EOL} denotes the number of cycles for which the capacity reaches the battery end of life EOL threshold (80 % of the initial capacity), t_{nom} - represents the number of cycles for the nominal capacity.

Figure 1 illustrates the interrelation between three key performance indicators of a lithium-ion battery: SoC (State of Charge), SoH (State of Health), and RUL (Remaining Useful Life), as presented in the study [21]. SoC represents the current level of available capacity relative to the nominal value, indicating the battery’s instantaneous energy readiness. SoH reflects the degree of battery degradation, decreasing progressively during cyclic operation. RUL denotes the predicted number of cycles until the end of life (EoL) is reached, when SoH falls below the acceptable threshold. The combined analysis of these indicators provides a comprehensive assessment of both the current and the forecasted condition of the battery.

Existing approaches reported in the literature typically operate on isolated battery health indicators-such as SoC, SoH, RUL, internal resistance, and so forth. However, this methodology is insufficient for comprehensive forecasting and real-time decision-making under the dynamic conditions of complex missions, where the integration of multiple parameters into a single metric is critically important.

By combining SoC, SoH, and RUL into a unified descriptor-such as the Dynamic Vector Efficiency (DVE)-one obtains a metric of the form:

$$DVE(t) = \frac{SoC(t) \cdot RUL(t)}{R_{int} \cdot T}, \quad (5)$$

where R_{int} – denotes the internal resistance of the battery (Ohm), T -represents the battery temperature (°C).

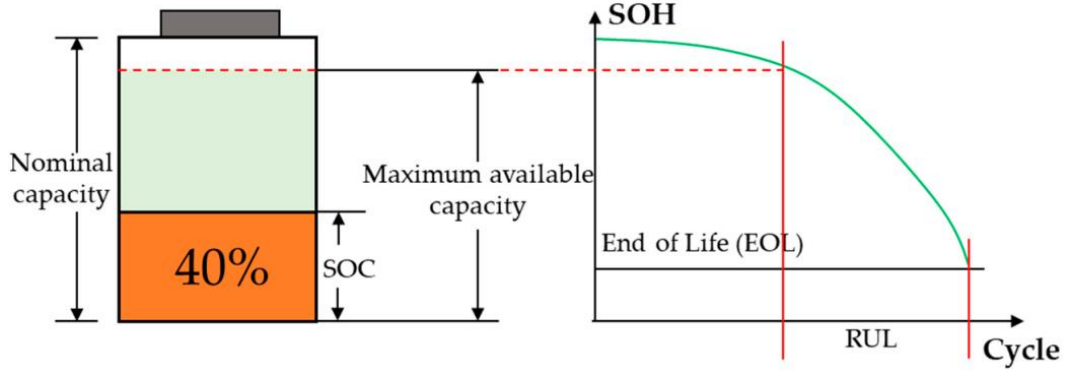


Figure 1: Interdependence of SoC, SoH, and RUL in Lithium-ion Batteries

The DVE is a dimensionless index that quantitatively characterizes the energy efficiency of a battery at a given moment by accounting for its SoC, RUL, and losses due to internal resistance and thermal effects. This enables MAS agents to rapidly assess the battery's condition by integrating both short-term and long-term indicators into a single numerical expression.

2.2. Construction of the Integral Health Vector

In order to standardize the parametric representation of the battery at each time t , we propose to construct an integral health vector – here after referred to as the Battery State Index Vector (BSIV) - which, in its most general form, is expressed as:

$$\vec{b} = [\text{SoC}(t), \text{SoH}(t), \text{RUL}(t), R_{\text{int}}, T, V_{\text{load}}, I_{\text{load}}, Z(f_1), \dots, Z(f_n)], \quad (6)$$

where $\text{SoC}(t)$ denotes the state of charge at time t ; $\text{SoH}(t)$ - the state of health (remaining resource) of the battery; $\text{RUL}(t)$ - Remaining Useful Life (number of cycles until the critical SoH); $R_{\text{int}}(t)$ - is the internal resistance of the cell (Ohm); $T(t)$ is the cell temperature at time t ($^{\circ}\text{C}$ or K), $V_{\text{load}}(t)$, $I_{\text{load}}(t)$ denote the voltage and current under load (V , A); $Z(f_i)$, $i=1, \dots, n$ - is the complex impedance measured at frequency f_i (Hz).

This vector may serve as the foundation for classification, prediction, and embedding projections. Its flexibility lies in the ability to incorporate additional parameters (e.g., $\frac{\Delta \text{SoC}}{\Delta t}$, enclosure temperature, degradation index, etc.).

The proposed integral health vector encapsulates all relevant information regarding the battery's current state. To enable effective detection of critical conditions, forecasting of degradation trends, and decision-making within a multi-agent environment, this vector is transformed into an embedding space of appropriate dimensionality. The objectives of this embedding representation are: information compression without loss of key features, cluster identification of battery states exhibiting similar characteristics, decision-space construction for energy-management agents, critical-zone detection based on threshold distances (Critical Distance Metric - CDM). For example, based on the embedding representation, one may introduce a novel metric that quantifies the Euclidean distance from the embedding vector \vec{b}_t to the critical-state region $\vec{b}_{\text{threshold}}$ (7):

$$\text{CDM}_t = \min_{\vec{b}_t} \|\vec{b}_t - \vec{b}_{\text{threshold}}\|. \quad (7)$$

Moreover, the embedding space derived from the integral health vector enables a transition from individual numerical parameters to a geometric interpretation of the battery's condition. Each

point within this space represents a unique state profile, and the distance between points correlates with the similarity of their technical conditions. This framework allows agents not only to classify the current state as normal or critical but also to detect degradation trends and latent anomalies in the distribution. Isolated features-such as SoC or the internal resistance R_{int} treated independently in classical methods, whereas the embedding space reveals nonlinear interdependencies among features that are not apparent in the raw data.

To reduce the dimensionality of the embedding space and construct a topologically meaningful representation, several approaches are commonly employed, including Principal Component Analysis (PCA) for linear compression and visualization, t-Distributed Stochastic Neighbor Embedding (t-SNE) or Uniform Manifold Approximation and Projection (UMAP) for nonlinear cluster separation, autoencoders for representation learning via reconstruction, and neural embedding layers (implemented via multilayer perceptrons) when the embedding is an integral part of the trained model. The application of PCA, autoencoders, or t-SNE facilitates the discovery of latent clusters-for example, groups of battery cells exhibiting similar aging rates or operating conditions. Forecasting the battery's future state within the PCA space is performed by leveraging clustering results in conjunction with a predictive model that projects the state at time $t+1$ (Figure 2).

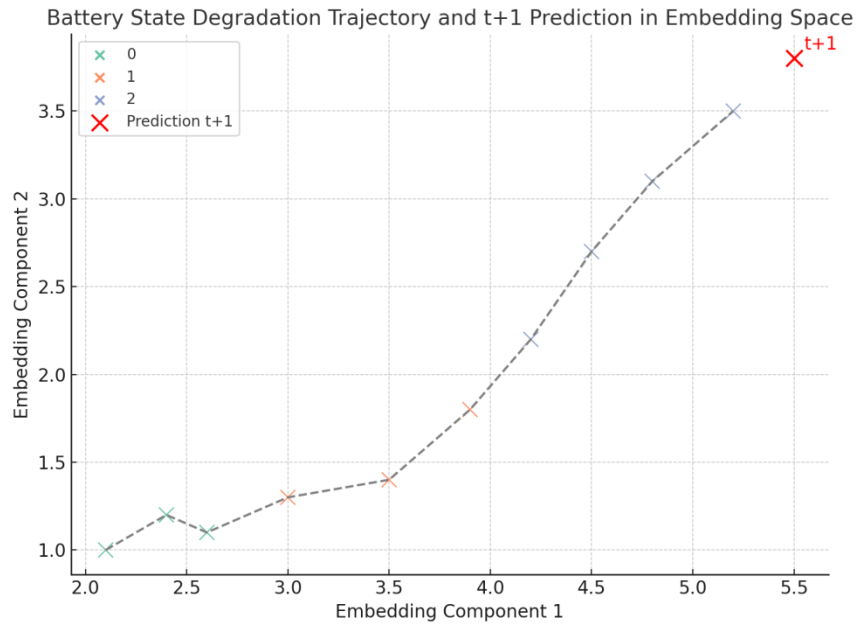


Figure 2: Forecasting the battery's future state within the PCA space

Despite the flexibility of the embedding-based approach, the accuracy of forecasting the battery's future state largely depends on the availability of high-quality, complete, and balanced datasets. In the event of insufficient sample representativeness or sudden changes in operating conditions, the embedding space may shift, adversely affecting classification and decision-making. Moreover, deep neural networks (in particular autoencoders, MLPs, and LSTMs) require careful hyperparameter tuning and are prone to overfitting when trained on limited data. At the same time, adapting these models for field deployment necessitates edge implementations with constrained computational resources.

The embedding space can serve as a generalized map of battery states for the entire system. Agents within the MAS analyze positions relative to clusters, forecast state-transition trajectories over time, and apply thresholding mechanisms based on Euclidean or cosine distances. They then optimize task allocation - such as repositioning or load distribution - across a UAV swarm. This approach combines local interpretability with global coherence in decision-making within the multi-agent architecture.

3. Implementation of the Multi-Agent Energy Management System

Based on the integral health vector described in the preceding sections, we propose an implementation of a multi-agent system (MAS) that performs monitoring, forecasting, and decision-making for energy consumption in UAV swarms and UGV groups. The MAS leverages the embedding space of battery states as its coordination environment. It is architected according to principles of agent distribution, vectorized state representation, stream-oriented data processing, and flexible hardware deployment. Agent distribution entails that each agent executes one or more functions within a clearly defined zone of responsibility. Under the vectorized state representation, all agents operate on a unified battery state vector.

3.1. Architecture of the MAS

The multiagent system comprises five distinct agent types-Sensor Agent, Embedder Agent, Classifier Agent, Predictor Agent, and Decision Agent-whose roles are detailed in Figure 3. The Sensor Agent acquires battery parameters (voltage, current, temperature, impedance) via SMBus, CAN, and I²C protocols and packages them as raw data. The Embedder Agent transforms this raw data into a state-feature embedding, which the Classifier Agent then uses to categorize the battery's condition as normal, degraded, or critical-employing techniques such as K-means clustering or decision trees.

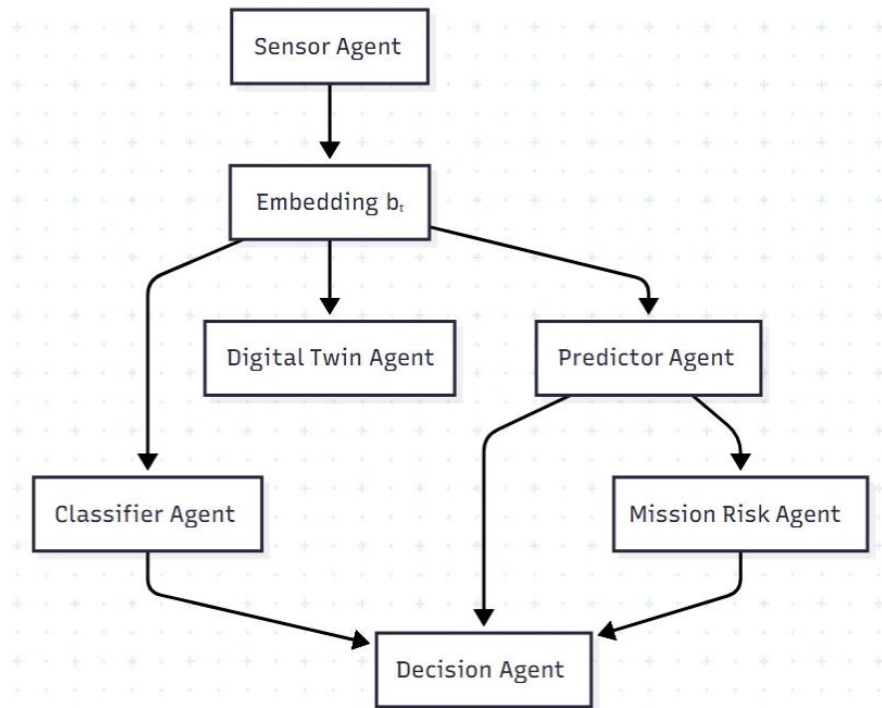


Figure 3: Architecture of the MAS

The Predictor Agent leverages the embedding trajectory to forecast future battery states and quantify associated risks, while the Decision Agent uses the classifier's output and risk assessment to adjust mission parameters-such as rerouting, load redistribution, or replacing drones in the swarm due to impending battery depletion.

As illustrated in Figure 3, the agent interaction algorithm proceeds as follows. The Sensor Agent periodically queries the battery's BMS module and logs into the "raw data" packet the instantaneous values of voltage, current, temperature, internal resistance, frequency-domain impedance, and additional relevant parameters. If data frames are missed or noise is excessive, the agent applies an internal smoothing filter (e.g., EMA or EKF). The Embedder Agent then consumes

this raw data, computes derived metrics (SoC, SoH, RUL, $\frac{dT}{dt}$, etc.), and constructs the integral state vector \vec{b}_t . This vector is normalized and projected into the embedding space using techniques such as PCA, autoencoders, or UMAP. The agent publishes the resulting embedding coordinates \vec{e}_t via a message queue (e.g., MQTT [15] or ZeroMQ) to the downstream agents.

For state classification, the Classifier Agent receives and assigns it to one of the predefined clusters-“Healthy,” “Warning,” or “Critical”-using methods such as K-means, hierarchical decision trees, or a Critical Distance Metric threshold. The classification outcome is then published along with a timestamp and confidence level. Predictor Agent The Predictor Agent generates a short-term forecast by maintaining an up-to-date predictive model (e.g., MLP, LSTM, or transformer) and predicts the battery’s forthcoming state \vec{e}_t . The Predictor Agent projects the battery’s future state over a specified “event horizon” (e.g., 1–5 min). If the predicted embedding falls within the critical region ($CDM < \epsilon$), the agent sets a “risk flag.” For decision-making, the Decision Agent ingests the current health classification, the risk flag, and mission context (e.g., distance to target, availability of spare drones, weather conditions, terrain/elevation data, tactical situation). Based on these inputs, it selects one of several action protocols-such as entering an energy-saving mode, rotating platforms within the swarm, or initiating an emergency return to the launch point.

Regarding the interaction of optional agents, it should be noted that the Digital Twin Agent initiates an update of the degradation model within the cloud-based digital twin, compares the actual and simulated trajectories $\vec{e}_{t,t+k}$ and transmits corrections to the Embedder and Predictor Agents. The Mission Risk Agent assesses the impact of energy loss on mission success-considering factors such as distance to target, remaining munitions, and time windows-ranks the associated risks, and, if necessary, elevates the priority of the Decision Agent.

During MAS operation, mechanisms for continuous feedback and self-updating must be ensured. All agents record their activities and telemetry data in a central log. Key performance metrics, such as prediction MAE and the percentage of critical deviations, are periodically reviewed. When the Predictor Agent’s accuracy degrades, it initiates automated retraining with the newly acquired data, while the Classifier Agent recalculates its clusters. This continuous feedback and self-update loop ensures the MAS adapts over time to maintain decision-making fidelity. Data exchange is performed via a publish–subscribe bus (e.g., MQTT), or over an embedded Ethernet network (e.g., EtherCAT or MIL-STD-1553B) in combat UGVs. Implementation on edge devices is feasible, provided that each agent is deployed as an autonomous container or process on an edge-compute module (e.g., Raspberry Pi, Jetson Nano, or other platforms as specified in [22]), with the capability to execute PyTorch Lite or MicroPython code. This ensures low latency and autonomous decision-making onboard the platform.

3.2. Example of MAS Application

In the simulation, a 40-minute flight scenario of a quadrotor UAV was employed under variable ambient temperatures ranging from +10 °C to –5 °C. The corresponding data are presented in Table 1. Based on the computed state vectors, embeddings, and the critical-distance threshold ($CDM < 0.15$), the agents identified the onset of a critical battery state after 36 minutes of flight.

Table 1
Hypothetical Battery State Vector Values at Selected Flight Times

t (min)	SoC	SoH	RUL	Rint (Ωm)	T (°C)	DVE	CDM
0	1.00	1.00	40	0.015	+10	66.7	1.20
10	0.80	0.99	30	0.017	+5	47.0	0.82
20	0.65	0.97	22	0.019	0	37.1	0.50
30	0.45	0.95	12	0.021	–2	25.7	0.27
36	0.31	0.94	6	0.025	–5	19.6	0.14

This example illustrates the application of multi-agent logic based on embedding vectors to provide real-time alerts of unacceptable battery states. Table 2 provides a structured comparison of the key characteristics of conventional battery-state assessment methods versus the innovative embedding-based approach proposed in this work.

Table 2
Comparison of Embedding-Based and Traditional Approaches

Criterion	Traditional Methods	Embedding-Based Approach
Input Data Type	Individual parameters only (SoC, internal resistance, temperature)	Multidimensional vectors combining SoC, SoH, RUL and other diagnostic features
Criticality Assessment	Rigid threshold rules, valid only within predefined scenarios	Geometric analysis in embedding space (cluster- and distance-based) allowing adaptive anomaly/critical-state detection
Forecasting Capability	Empirical formulas or instantaneous diagnostics	Integrated ML-driven forecasting (MLP, LSTM, transformer) supporting short- and medium-term degradation prediction
Scalability	Typically tailored to single platforms or requires significant re-engineering for swarms	Naturally scalable - identical embedding model can serve swarms of UAVs/UGVs while accommodating individual device profiles
Adaptation to New Conditions	Manual recalibration or re-tuning	Online model adaptation (retraining, cluster re-computation) driven by telemetry feedback
Edge Deployment & Real-Time Usage	Varies; may need high-performance hardware for on-board ML	Designed for edge containers/processes on lightweight compute modules (e.g., Raspberry Pi, Jetson Nano) running PyTorch Lite or MicroPython with low latency
Interpretability & Decision Logic	Limited to individual metrics	Embedding vectors provide both local interpretability (via distance/cluster metrics) and global consistency for multi-agent decision protocols
Integration with Digital Twins	Often standalone, manual data exchange	Direct feedback loops with cloud-based digital twins for automatic calibration and continuous refinement of both the embedding and degradation models

In terms of input data type, traditional methods are limited to individual parameters-such as State of Charge (SoC), internal resistance (R_{int}) and temperature-which do not capture the holistic dynamics of degradation. By contrast, the embedding approach operates on vectors that unify multiple parameters-including SoC, State of Health (SoH), Remaining Useful Life (RUL), and additional diagnostic features-thereby creating a unified, multidimensional representation.

Regarding criticality assessment, classical techniques employ rigid threshold rules that are informative only within predefined scenarios. In opposition, the embedding method relies on geometric analysis within the vector space, enabling anomaly detection, cluster formation of battery states, and recognition of complex nonlinear relationships.

From a scalability perspective, traditional approaches are generally tailored to single platforms or require significant adaptation to scale. Embedding representations, on the other hand, are inherently scalable and allow a single model to be applied efficiently across a swarm of UAVs or UGVs, while still accommodating the individual characteristics of each device.

When comparing forecasting capabilities, classical methods are often confined to instantaneous diagnostics or the application of empirical formulas, whereas the embedding-based approach supports integrated machine learning-driven prediction mechanisms. This enables the anticipation of degradation trajectories over time. Finally, in the context of adaptation to new operating

conditions, traditional solutions require manual retuning or recalibration, whereas the embedding methodology allows for online model adaptation, thereby maintaining dynamic alignment with evolving environmental factors and individual usage profiles. Overall, the foregoing analysis underscores the advantages of the embedding-based approach in meeting the contemporary demands of autonomous energy systems.

4. Conclusion

In this work, an embedding-based approach to implementing a multi-agent energy management system for unmanned platforms was examined. The proposed representation of the battery's state as a feature vector \vec{b}_t in a multidimensional embedding space enables the implementation of powerful real-time classification, prediction, and decision-making capabilities.

The study demonstrates the effectiveness of clustering battery state vectors for early detection of critical operating modes, confirms the feasibility of short-term degradation forecasting with acceptable accuracy using an MLP model, develops a multi-agent system architecture with clearly delineated roles for Sensor, Classifier, Predictor, and Decision agents that can be deployed on edge devices, establishes the potential for integration with battery digital twins to simulate cell behavior under dynamic mission conditions, and provides a comparative analysis of the embedding-based approach versus traditional battery-state assessment methods. The obtained results indicate the advisability of employing embedding-based models for energy monitoring tasks in autonomous systems, particularly in scenarios where reliability and predictability of power supply are critical. The proposed approach is scalable, adaptive, and enables the extension of multi-agent system functionality under constrained computational resources. Further research in this area may focus on several key directions:

Expanding datasets and simulations by collecting large volumes of real flight and mission data to train and validate embedding models under operational (combat) conditions-taking into account temperature, load profiles, and climatic scenarios-and on integrating with digital twins of power systems by developing mechanisms for automatic model calibration based on feedback from physical or virtual battery instances within the digital twin framework.

The development of an interactive decision space-including the creation of a visual representation of the embedding space for operators or command systems, complete with built-in risk assessment and scenario modeling capabilities constitutes another promising direction; equally important is the exploration of heterogeneous agent systems, extending the multi-agent architecture with hybrid agents that combine rule-based control and reinforcement learning. Addressing scalability and adaptation across diverse platform types-from first-person-view (FPV) drones and lightweight ground vehicles to Class II and III UAVs with redundant power circuits will be critical for deploying these methods in real-world operational contexts. This prospect paves the way for the development of fully adaptive decision-support systems for tactical and operational energy-management in autonomous combat platforms.

Declaration on Generative AI

During the preparation of this work, the author(s) used GPT-4 and DeepL in order to: DeepL and spelling check. Further, the author(s) used GPT-4 for figure 2 in order to: for the purpose of generating images using synthetic data. After using these tool(s)/service(s), the author(s) reviewed and edited the content as needed and take(s) full responsibility for the publication's content.

References

- [1] M. Murnane, A. Ghazel, A Closer Look at State of Charge (SOC) and State of Health (SOH) Estimation Techniques for Batteries. 2023. URL:

- <https://www.analog.com/en/resources/technical-articles/a-closer-look-at-state-of-charge-and-state-health-estimation-tech.html>.
- [2] W. Li, M. Rentemeister, J. Badedae, D. Jösta, D. Schulte, D. Uwe Sauer, Digital twin for battery systems: Cloud battery management system with online state-of-charge and state-of-health estimation. *Journal of Energy Storage* (2020). doi:10.1016/j.est.2020.101557
 - [3] B. Saha, K. Goebel, Battery Data Set. NASA Ames Prognostics Data Repository. (2009) <https://www.nasa.gov/content/prognostics-center-of-excellence-data-set-repository>
 - [4] Berezovskyi, A., et al. Interpretable neural networks for battery health prediction. *Energy AI*, 7 (2022) 100135.
 - [5] K. Liu, K. Li, Q. Peng, C. Zhang, A brief review on key technologies in the battery management system of electric vehicles. *Frontiers in Mechanical Engineering*, 5 23 (2020).
 - [6] X. Zhang, J. Jiang, C. Zhang, et al., Remaining Useful Life Prediction of Lithium-ion Batteries Based on Neural Network Embedding Space. *IEEE Access*, 9, 2021, pp.72147–72156.
 - [7] B. Sun, et al.: Energy efficient cooperative mission planning for drone fleets with battery constraints. *Journal of Field Robotics*, 38 4 (2021) 524–543.
 - [8] S. M. Lundberg, S.-I. Lee, A Unified Approach to Interpreting Model Predictions. *Advances in Neural Information Processing Systems*, 30 (2017).
 - [9] J. Kim, B.H. Cho, State-of-charge estimation using a neural network with adaptive learning rate for a lithium-ion battery. *IEEE Transactions on Vehicular Technology*, 60(1), 2011, pp.296–308.
 - [10] S. Han, et al. Real-time Battery Degradation Prediction using Edge AI and Transfer Learning. *Sensors*, 23 (2) (2023) 521.
 - [11] S. Hochreiter, J. Schmidhuber, Long short-term memory. *Neural Computation*, 9 8 (1997) 1735–1780.
 - [12] A. Vaswani, et al. Attention is All You Need. *Advances in Neural Information Processing Systems*, 30 (2017).
 - [13] K. He, X. Zhang, S. Ren, J. Sun, Deep residual learning for image recognition. *CVPR 2016*, 770–778.
 - [14] R. Zhao, et al. Review on modeling of lithium-ion battery for EV battery management system. *CSEE Journal of Power and Energy Systems*, 6 1 (2020) 19–30.
 - [15] V. Slyusar, Distributed Multi-agent Systems Based on the Mixture of Experts Architecture in the Context of 6G Wireless Technologies. In: Dovgyi, S., Siemens, E., Globa, L., Koptika, O., Stryzhak, O. (eds) *Applied Innovations in Information and Communication Technology. ICAIT 2024. Lecture Notes in Networks and Systems*, vol. 1338, 2025, Springer, Cham. doi:10.1007/978-3-031-89296-7_6.
 - [16] V. Slyusar, V. Kozlov, S. Pochernin, I. Nalapko, Conceptual foundations of the swarm employment of unmanned aerial vehicles as intelligent means of electronic warfare. *Technology Audit and Production Reserves*, 3 2 83 (2025) 71–80. doi:10.15587/2706-5448.2025.329989.
 - [17] O. Kozlov, I. Sidenko, O. Gnatyuk and O. Korchenko, Intelligent UAV control system based on the Internet of Things for meteorological measurements, *Journal of Mobile Multimedia* 20 3 (2024) 555–596,. doi: 10.13052/jmm1550-4646.2032.
 - [18] I. Sidenko, O. Kozlov, O. Gnatyuk and O. Korchenko, Machine learning for unmanned aerial vehicle routing over rough terrain, in: *Advances in Computer Science for Engineering and Education VI*, Z. Hu, I. Dychka, and M. He, Eds., *Lecture Notes in Data Engineering and Communication Technologies*, vol. 181, 2023, pp. 626–635. https://doi.org/10.1007/978-3-031-36118-0_56.
 - [19] M. A. Hannan, M. S. H. Lipu, M. H. M. Saad and A. Hussain, Enhanced capacity estimation of lithium-ion batteries using adaptive extended Kalman filter and recursive least squares. *Batteries* 9 2 (2023) 131. doi:10.3390/batteries9020131.

- [20] Z. Zhu, Q. Yang, X. Liu and D. Gao *Attention-based CNN-BiLSTM for SOH and RUL estimation of lithium-ion batteries*. Journal of Algorithms & Computational Technology 16 (2022) 2-3. doi:10.1177/17483026221130598.
- [21] J. Zhao, Y. Zhu, B. Zhang, M. Liu, J. Wang, C. Liu, X. Hao, Review of State Estimation and Remaining Useful Life Prediction Methods for Lithium-Ion Batteries. Sustainability, 15 (6) (2023). 5014. doi:10.3390/su15065014.
- [22] V. Slyusar, Y. Kondratenko, A. Shevchenko, T. Yeroshenko, Some Aspects of Artificial Intelligence Development Strategy for Mobile Technologies. Journal of Mobile Multimedia 20 3 (2024) 525–554. doi:10.13052/jmm1550-4646.2031.